DAMPING OF SOIL BY CROSS-HOLE METHOD

DAMPING DU SOL AVEC LA METHODE CROSS-HOLE

Claudio Mancuso

Researcher, Istituto di Tecnica delle Fondazioni e Cotsruzioni in Terra (Geotecnica)
University of Naples *Federico II*, Naples, Italy

SYNOPSIS: At the *Istituto di Geotecnica* of the *University of Naples Federico II* some theoretical and experimental studies have been carried out for the analysis and application of cross-hole (*CH*) in-situ *damping* measurements. Theoretical studies have been focused on the spectral analysis of simulated seismic waves and have allowed the understanding of the limitation and effectiveness of *damping* measurement technique. Multi-receivers *CH* tests have been next accomplished in the core material of the Bilancino dam (Italy) and in-situ results have been compared with resonant column-torsional shear measurements performed on undisturbed samples of the same material. The outcomes of this study, summarized in the paper, bring out a good agreement between in-situ and lab *damping* measurements for this soil and highlight some peculiarities of its behaviour.

1. INTRODUCTION

Beyond the usual measurements of shear and compressional soils stiffness, the cross-hole (*CH*) method can also be used to evaluate *damping* (Sanchez-Salinero *et. al.*, 1986; Sanchez-Salinero, 1987; Mok, 1987; Mancuso and Silvestri, 1991; Mancuso, 1992). In fact, the body waves delivered at the *CH* source will reduce their amplitude because both the wave-front expansion and energy *absorption* by the medium itself; thus, according to source distance the recorded wave-form will modify, the amplitude reducing and time lag between consecutive wave peaks increasing. It is then plain trying to measure soil *damping* (*D*) by *CH* wave-forms analysis, provided that more than one receiver lined up to the source is used.

CH damping evaluation require Fourier decomposition of 2 body waves records, single out the amplitudes and phase shift stored over the receivers travelling-path by each Fourier component (harmonic) and recognition of the source-receivers spacing; the first two quantity are the *Spectra Magnitude* and *Cross Power Spectrum Phase* of the recorded signals while the third require inclinometer measurements.

Unfortunately, *CH* amplitude measurements suffer of various problems, the more important one being: *a* - environmental noise effects; *b* - hole casings and receivers coupling interference; *c* - direct and refracted waves interaction; *d* - *near field* contribution to the recorded motion (Sanchez-Salinero, 1987; Mancuso and Vinale; 1987, 1988 [a]).

a - The noise effect can be reduced to an acceptable threshold by precise transducers calibration, use of differential amplifiers (Mancuso *et. al.*, 1988, 1989), shielding of signal cables, digital filtering. Regardless these hints, amplitude monitoring can be contaminated by a differential receivers response due to their axis deviation (hole curvature).

b - Variation in the receivers-casing reaction can generate another transducer response alteration. Though the direct verification of the coupling system performances is recommendable (Mok, 1987), it seems reasonable assuming that repetitive casing installation and pneumatic (controlled pressure) receivers coupling system can give a sufficiently uniform response in homogeneous soils.

c - The procedure needed for direct and refracted waves interference reduction is widely discussed in literature (Mok *et. al.*, 1988; Mok 1987) and consist in signals windowing. The basic hypothesis is that in the time history of a point motion the first recorded oscillation is free of refracted terms and hence due only to direct waves; therefore weighing can be used to isolate the direct waves signal part. However, because weighing effect is influenced by the source-receiver distance, in the experimental *CH* measurements elaboration presented below it was preferred not to perform any signal windowing (the almost uniform stiffness of the experienced soil give rise to a small effect of refracted waves).

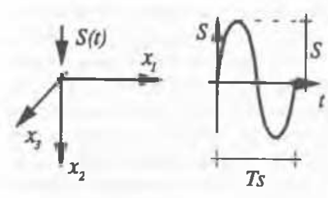

Fig. 1. The loading function.

d - For the analysis of the interaction between *near field* and *far field* terms some further studies have been carried out, in addition to the available ones (Sanchez-Salinero *et. al.*, 1986; Sanchez-Salinero, 1987). A brief discussion of the model adopted and results obtained are presented in the following section.

2. ANALYSIS OF SYNTHETIC *CH* RECORDS

In the *CH* method the body waves delivered by a directional source are recorded by receivers (velocity transducers) placed at the same depth of the source. Usually the recorded vibrations are due both to direct and refracted waves, but, if the propagation medium stiffness is almost uniform or the source-receivers spacings are properly selected with respect to the tested soil strata thickness, the effect of direct waves will prevail. In such a conditions the wave-form characteristics are essentially the same as for an unbounded medium.

Furthermore, the strain levels involved in the *CH* tests are very small (generally $\gamma < 10\text{-}5 \div 10\text{-}6\%$) and hence the propagation media can be regarded as a linear elastic continuum.

Under these hypotheses it is plain modelling *CH* measurements as wave propagation in an elastic, homogeneous space, in witch the displacement $u(x,t)$ observed in a point x can be expressed as:

$$u(x,t) = S(t) * H(x,t) * I(t)$$

with: $S(t)$ a source loading function; $H(x,t)$ and $I(t)$ the propagation medium and receiver transfer function; (*) the convolution operator.

Alternatively, $u(x,t)$ can be expressed by its frequency domain equation:

$$u(x,\omega) = S(\omega)\,H(x,\omega)\,I(\omega)$$

and by superimposition of its Fourier terms $u(x,\omega)$.

2.1 CH network response

The ***source loading function*** utilized in this study consists (see *Fig. 1*) in a pulse applied at the origin of the reference system (x_1, x_2, x_3) and acting along the j axis; the loading function $S_j(t)$ shape is a sine cycle of amplitude S. In spite the loading history is not harmonic, the time lag between its onset and complete decay will be next named *source fundamental period* (T_s) while *source fundamental wavelength* λ_s will be T_s times the shear wave velocity $\beta=\sqrt{(G/\rho)}$ (G shear stiffness and ρ density of the elastic continuum). Furthermore, the function $S(\omega)$ will be obtained by the Fourier transform of $S(t)$.

In a linear elastic, homogeneous, isotropic space and for an x_j directional source, the ***propagation medium transfer function*** or ***Green function*** (solution of the steady state problem) is:

$$H_{ij}(x,\omega)=\frac{e^{-i\omega r/\alpha}}{4\pi\rho\alpha^2 r}[\gamma_i\gamma_j+(3\gamma_i\gamma_j+\delta_{ij})(\frac{\alpha}{i\omega r})+ +(3\gamma_i\gamma_j-\delta_{ij})(\frac{\alpha}{i\omega r})^2]+ -\frac{e^{-i\omega r/\beta}}{4\pi\rho\beta^2 r}[(\gamma_i\gamma_j-\delta_{ij})+(3\gamma_i\gamma_j-\delta_{ij})(\frac{\beta}{i\omega r})+ +(3\gamma_i\gamma_j-\delta_{ij})(\frac{\beta}{i\omega r})^2] \qquad [1]$$

with: r the source-receiver distance, α and β the compressional an shear wave velocities, γ_k the source-receiver spacing direction cosine in the loading direction x_j and explored displacement component (u_i), i the imaginary unit, ω the circular frequency and δ_{ij} the Kronecker delta.

The *Green function* is then a summation of two constant frequency waves propagating with the shear and compressional velocities. Each wave is composed by $1/r$, $1/r(\lambda/r)$ and $1/r(\lambda/r)^2$ rank addenda, where λ is equal to $\lambda_\alpha=\alpha/f$ or $\lambda_\beta=\beta/f$ (shear and compression wavelength) and $1/(\lambda/r)$ is the number of wavelengths contained in r. Therefore, the magnitude of the various terms of equation *[1]* depends upon r and λ; if λ is larger than r (greater then $r/2$ according to Sanchez-Salinero *et. al.*, 1986) the $1/r(\lambda/r)$ and $1/r(\lambda/r)^2$ factors will be significant and, on the contrary, if λ is small enough $1/r$ will be predominant. This is the reason why the first two terms are referred as *near field* (λ and f will are *near field wavelength* and *frequency*) and the terms $1/r$ are called *far field*. It seems interesting to note that soils α and β and actual source-receivers spacing can turn in an remarkable effect of *near field* terms in some commonly used *CH* frequency range.

A time domain transient pulses can be reproduced by its Fourier components superimposition just in the case of elasticity, while in this study we have to simulate an energy absorbing material. We bypass this difficulty introducing the complex stiffness in formula *[1]*:

$$G^* = G(1 + 2iD)$$

where D (*damping ratios* or *damping*) represents the absorbed strain energy normalized with respect to the one stored in the first monotonic loading.

In the *CH* method displacements are monitored by ***receivers*** (velocity transducers) with their own ***transfer function***. Their filtering action has been here simulated by the following equation:

$$I(\omega) = \frac{(\frac{\omega}{\omega_1})^2}{[1-(\frac{\omega}{\omega_1})^2+2i\mu\frac{\omega}{\omega_1}]\,[1-(\frac{\omega}{\omega_2})^2+2i\mu\frac{\omega}{\omega_2}]}$$

where $\mu=0.5$ is the damping of the transducer and $\omega_2/\omega_1=20$ corresponds to a cut-off frequencies ratio (*-6dB* signal reduction) equal to *50*.

2.2 Damping evaluation

To quantify *damping*, we must eliminate from $u(x,\omega)$ equation the wave amplitude reduction due to the geometrical spread of energy. In spite to the

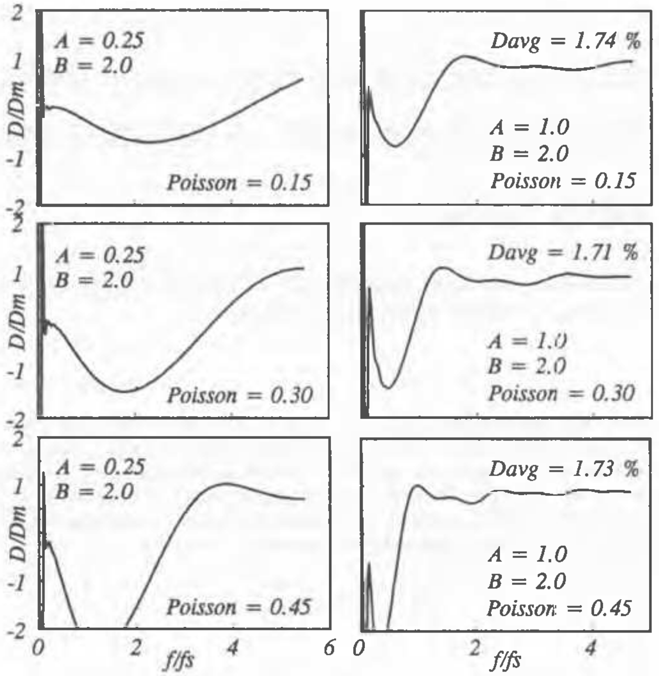

Fig. 2. Near field damping ($r_1/\lambda_s=0.25\div1.0$, $r_2/r_1=2.0$).

presence of both *near field* and *far field* terms and because the *near field* contribution vanish at large r, it was decided to approximated the geometrical spread by the following formula (Aki and Richards, 1980):

$$A_2(f) = A_1(f)\,\frac{r_1}{r_2}$$

with A_i displacement amplitudes at two r_i source-spaced points.

Introducing the model *absorption* of energy, the amplitude $A_2(f)$ expression obtained is (Bornoitz, 1931):

$$A_2(f) = A_1(f)\,\frac{r_1}{r_2}\,e^{-\zeta(r_2-r_1)}$$

with ζ (*material damping*) the *absorption* of energy by the medium itself.

By the relation between *logarithmic decrement* Δ, ζ and *damping*;

$$\Delta = \frac{\zeta\,V(f)}{f}\,, \qquad D = \sqrt{\frac{\Delta^2}{4\pi^2 + \Delta^2}}$$

and using the previous equation for ζ, D can be expressed as:

$$D(f) = \frac{\ln\frac{A_1(f)r_1}{A_2(f)r_2}}{\sqrt{(2\pi t_{12} f)^2+[\ln\frac{A_1(f)r_1}{A_2(f)r_2}]^2}}$$

Moreover, in the *CH* an harmonic wave travel-time (t_{12}) between two X spaced points is:

$$t_{12} = \frac{X}{\Delta\phi(f)/2\pi}f$$

where $\Delta\phi(f)$ is the phase shift between two source lined-up receivers.

Then, by a simple substitution, the *damping* formula became:

$$D(f) = \frac{\ln\frac{A_1(f)r_1}{A_2(f)r_2}}{\sqrt{\Delta\phi(f)^2+[\ln\frac{A_1(f)r_1}{A_2(f)r_2}]^2}} \qquad [2]$$

Equation *[2]* stresses the importance of accurate amplitude measurements for *damping* evaluation, being A_i the arguments of logarithmic functions.

2.3 *Near field effect*

As stressed in the introduction (see point *d*), a basic requirement of the *CH damping* measurement is to avoid the noise effect of the *near field* wave components. Furthermore, the equation *[1]* emphasizes the dependence of amplitude and time position of *near field* terms on λ_β/r and λ_α/r ratios. That is the A_i amplitudes can be strongly influenced by the actual λ/r; an apparent production of energy ($D<0$) between the recording stations can even be hold by the polarity opposition of the compression and shear *near field* waves (see eq. *[1]*) and by the use of equation *[2]*.

To study this problem, the analytical formulation previously introduced has been used for *CH* measurements simulation. According to the experimental technique, where velocity transducers are employed as probes, the dynamic response of two points of the "elastic" (energy absorbing) space has been expressed in terms of velocity. Furthermore, to simulate the actual acquisition method (digital data collection), a sampling rate Δt, a number of samples N and a time record length T_r suitable for the frequency domain analysis have been used. The values adopted and corresponding frequency resolution Δf and maximum frequency f_{max} are listed below:

$$N = 2^{10} = 1024$$
$$\Delta t \approx 0.04\,T_s$$
$$T_r = N\,\Delta t$$
$$f_{max} = 1/(2\Delta t) = 50 f_s$$
$$\Delta f = 1/(N\,\Delta t) \approx 0.1 f_s$$

with $f_s = 1/T_s$ source fundamental frequency.

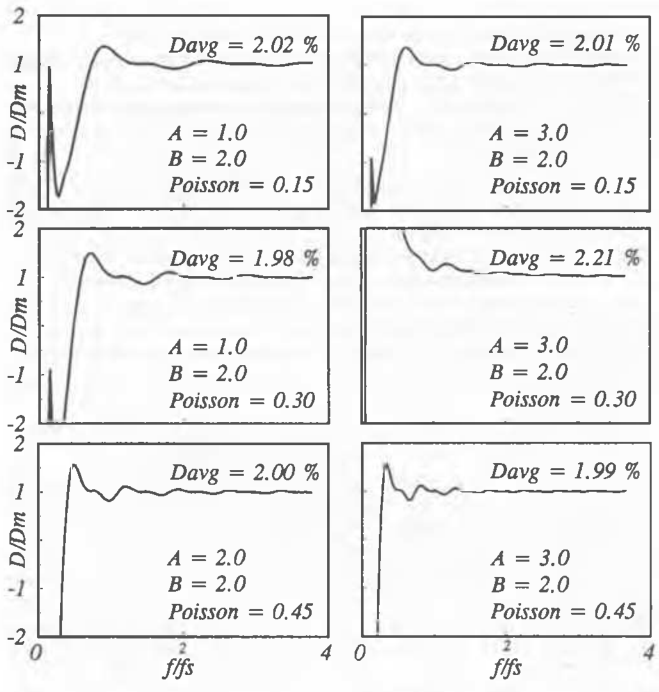

Fig. 3. *Far field* damping ($r_1/\lambda_s = 2.0 \div 3.0$, $r_2/r_1 = 2.0$).

The model parameters have been fixed considering the influence of the Poisson's ratio ν on both the time position of shear *far field* and *near field* compressional terms (α and β ratio depend upon ν); either *0.15* or *0.30* or *0.45* space Poisson's ratio have been used. Model *damping* has been fixed equal to 2%, while, because of the dependence of the solution on α/β and λ_s/r ratios, stiffnesses needs not to be specified.

The simulation refers to the *CH* shear stiffness experimental set-up, where source and receivers are at the same depth and the pulse is orthogonal to the source-receivers array.

The results of the analysis have been normalized: dividing the actual frequency by the source fundamental one ($f_s = 1$) and the current *damping* value by the model one.

In *Fig. 2* results obtained using $r_1/\lambda_s = 0.25$ and *1.0* and $r_2/r_1 = 2.0$ are presented (in the figures r_1/λ_s and r_2/r_1 will be indicated as A and B respectively); three Poison's ratios values have been considered (*0.15*, *0.30* and *0.45*).
In the case $r_1/\lambda_s = 1/4$ no *far field frequencies* are excited and in all of the three presented cases *damping* versus frequency diagram does not reach a stable value; the measurement technique is ineffective.
In the case $r_1/\lambda_s = 1.0$ a large range of *far field frequency* exist and the *damping* plot looks quite stationary beyond the *near field frequencies* ($f/f_s > 2\lambda_s/r = 2.0$). This occurrence is misleading since the average value of *damping* D_{avg}, computed considering the *far field frequencies* only, is remarkably smaller than 2%; the scatter being *14.5÷13%* depending on Poisson's ratio.

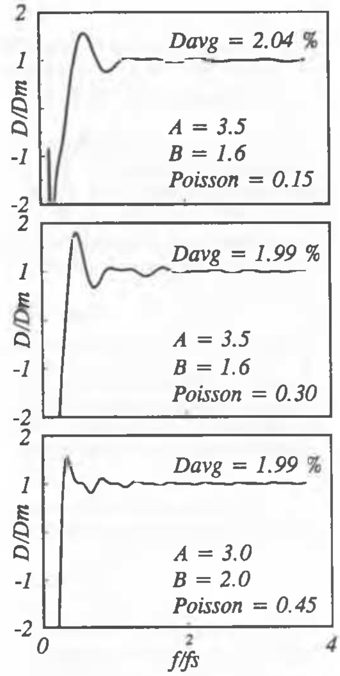

Fig. 4. *Far field* damping (r_1/λ_s= 3.5, $r_2/r_1 = 1.6$).

Two different cases, referred to $r_1/\lambda_s = 2.0$ and *3.0* (*far field*), are presented in *Fig. 3*; Poisson's ratios and r_2/r_1 are the same as *Fig. 2*. The *damping* plots are rapidly stabilized around the exact model value. Furthermore, using the average *far field* criterion for output *damping* evaluation, the percentile scattering to the model assigned values is really small in two cases but still large (*10.5%*) in the case of $r_1/\lambda_\beta = 3$ and $\nu = 0.3$. It is worth noting that in the former case the *damping* versus frequency plot is remarkably unstable also in the first part of the *far field* frequency range. Taking into account the only stable part of the plot the percentile scattering was reduced to the one observed in the other *far field* cases.

A good match between *far field* D_{avg} and model *damping* (D_m) has been also achieved by the source-receivers set-up identified with $r_1/\lambda_s = 3.5$ and $r_2/r_1 = 1.6$ (see *Fig. 4*); the percentile scattering between D_{avg} and D_m being smaller then 2%. It is interesting to note that the former geometrical arrangement is similar to the one used in the experimental measures discussed below.

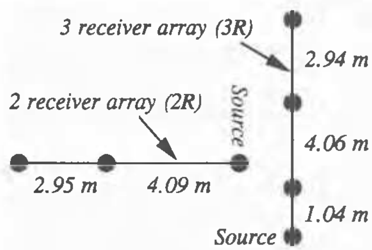

Fig. 5. *CH* stations plan view.

3. EXPERIMENTAL APPLICATIONS

The *Istituto di Geotecnica* of the *University of Naples "Federico II"* has recently carried out a field investigation program in witch the *CH damping* measurement technique has been tested; the work was a part of a leading experimental program for the characterization of the cyclic and dynamic behaviour of *Bilancino dam* core material. The leading program consists in *CH*, *down-hole* and *SASW* in-situ tests and *resonant column-torsional shear* (*RC-TS*) laboratory measurements (Silvestri, 1991) and allows the comparison between in-situ and lab results.

The soil type is classified as a medium plasticity *clayey and sandy silt* which physical properties are summarized in *Table I*.

In this soil *CH damping* measurements were performed using the *2* borehole arrays (for a total of *7* holes) schematically depicted in *Fig. 5*; in this way both *near field* and *far field* condition have been produced.

An example of experimental *far field CH damping* measurement is reported in *Fig. 6* (depth *17.0 m*); the *Power Spectra Magnitudes* at the *2 far field* receivers, their *Cross Power Spectrum Phase* and *damping* plots are shown. The *Power Spectra* shows that a considerably large amount of wave energy is stored in the frequency range $f_{min}=30 \div f_{max}=400\ Hz$; furthermore, the *damping* plot look very stable in the *far field* frequency range.

Table I - Average Characteristic of core material.

γ kN/m^3	γ_s kN/m^3	γ_d kN/m^3	w_0 %	e_0	S_{r0} %	w_{opt} %	w_l %	w_P %	I_P %	I_C %	CF %
20.0	26.5	17.5	18	0.56	87	14	43	23	20	1.25	25

The in-situ and lab results comparison ought to be done at the same mean effective stress p'. This might be calculated in-situ as:

$$p'=(\gamma z-u_c)\frac{(1+2k_o)}{3}$$

(γ unit weight and u_c un-saturated soils pore pressure), while as isotropic stress minus u_c in lab. Because of the effect of capillary tension is hard to quantify, it was decided referring to the *nominal mean stress (p)* defined as in the latter formula neglecting the u_c contribution. This hypothesis may not be a strong limit for in-situ and lab tests comparison.

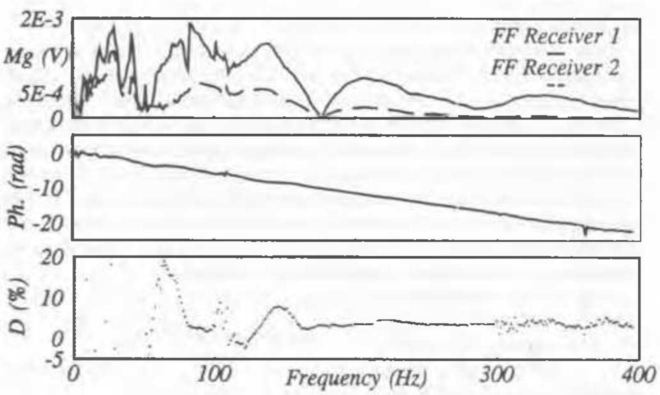

Fig. 6. Examples of damping measurements (depth *17.0 m* - *4* hole array).

The k_o value required for in-situ p evaluation has been estimated using the elasticity theory [$\nu/(1-\nu)$] and the compressional and shear wave velocity from *CH* measurements; an average k_o *(0.67)* have been obtained.

Results gained in all the *CH* and *RC damping* measurements are reported in *Fig. 7*. Two distinct trends as a function of p are evident; for p less then *150 kPa*, *damping* is inside the range *5%÷7%* while at larger p gradually drops to *3%*. The *damping* values are quite large and in good agreement with *RC* results.

4. CONCLUSIONS

From the theoretical studies here summarized it can be concluded that in *damping* measurements it is absolutely necessary placing receivers in the *far field* range; the source predominant frequency and soil shear wave velocity must then be predicted (source frequency might be regulated). The minimum acceptable r_1/λ_s value is 2; mismatching of this condition can turn in misleading results even in the simple case of an homogeneous, "elastic" space. On the contrary, equation *[2]* gives reliable results if both the receivers are in the *far field* range.

The experimental application of *CH damping* measurement technique has given good results, even if more scattered than lab one. The in-situ values seem to be a little larger the lab one: this could be due to differences in the loading rate. Nevertheless, the overall match between *CH* an *RC* tests states the effectiveness of *in-situ CH damping* measurements for almost uniform stiffness soils, even in the case of no signals windowing.

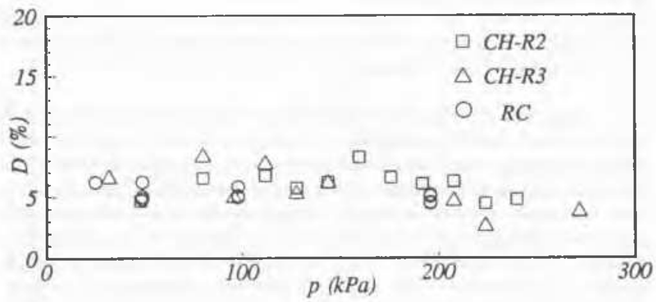

Fig. 7. In-situ and lab experimental results.

REFERENCES

AKI K, RICHARDS P.G. (1980). *Quantitative Seismology: Theory and Methods*, W.H Freeman Company, New York.

BORNOITZ G. (1931). *Uber Die Ausbretung Dor Von Agroszklbenmaschimen Erseugten Budenschwingungen Die Tiefe*, J. Springer, Berlin.

MANCUSO C. (1992). *Misura in Sito delle Proprietà dei Terreni mediante Prove Dinamiche*, Diss. di Dott., Univ. Napoli *Federico II*.

MANCUSO C., SILVESTRI F. (1991). *Rigidezza e Smorzamento di un Materiale da Nucleo Mediante Prove Dinamiche*, Gruppo Naz. di Coord. Studi Ing. Geot., Roma.

MANCUSO C., SIMONELLI A., VINALE F. (1988). *Misure di Velocità delle Onde di Taglio nella Piana del Fucino*, Gruppo Naz. Coord. Studi di Ing. Geot., Monselice, Padova.

MANCUSO C., SIMONELLI A., VINALE F. (1989). *Numerical Analysis of in Situ S-Wave Measurements*, Proc. XII ICSMFE, Rio de Janeiro.

MANCUSO C., VINALE F. (1987). *Un Modello per lo Studio della Propaga zione delle Onde Sismiche*, Gruppo Naz. Coord. Studi Ing. Geot., Roma.

MANCUSO C., VINALE F. (1988) [a]. *Propagazione delle Onde Sismiche: Teoria e Misura in Sito*, Gruppo Naz. Coord. Studi Ing. Geot., Monselice, Padova.

MOK Y.J. (1987). *Analytical and Experimental Studies of Borehole Seismic Methods*, Ph. D. Diss., The Univers. Texas, Austin.

MOK Y.J., SANCHEZ-SALINERO I, STOKOE K.H. II, ROESSET J.M. (1988). *In Situ Damping Measurements by Cross Hole Seismic Method*, II Spec. Conf. Earth. Eng. Soil Dyn., ASCE, Park City, Utah.

SANCHEZ-SALINERO I. (1987). *Analytical Investigation of Seismic Methods Used for Engineering Applications*, Ph. D. Diss., Univ. Texas, Austin, 1987.

SANCHEZ-SALINERO I., ROESSET J.M, STOKOE K.H II (1986). *Analytical Studies of Body Wave Propagation and Attenuation*, G.R.86-15, Univ. Texas, Austin.

SILVESTRI F. (1991). *Analisi del Comportamento dei Terreni Naturali in Prove Cicliche e Dinamiche di Taglio Torsionale*, Diss. Dott., Univ. Napoli *Federico II*.